Lawrence Berkeley National Laboratory

Title
On Two-Phase Relative Permeability and Capillary Pressure of Rough-Walled Rock Fractures

Permalink
https://escholarship.org/uc/item/5j291513

Authors
Pruess (ed), K.
Tsang, Y.W.

Publication Date
1989-09-01

Lawrence Berkeley Laboratory
UNIVERSITY OF CALIFORNIA

EARTH SCIENCES DIVISION

Submitted to Water Resources Research

On Two-Phase Relative Permeability and Capillary Pressure of Rough-Walled Rock Fractures

K. Pruess and Y.W. Tsang

September 1989

On Two-Phase Relative Permeability and
Capillary Pressure of Rough-Walled Rock Fractures

K. Pruess and Y. W. Tsang

Earth Sciences Division
Lawrence Berkeley Laboratory
1 Cyclotron Road
Berkeley, California 94720

September 1989

ON TWO-PHASE RELATIVE PERMEABILITY AND CAPILLARY PRESSURE OF ROUGH-WALLED ROCK FRACTURES

K. Pruess and Y. W. Tsang

Earth Sciences Division
Lawrence Berkeley Laboratory
1 Cyclotron Road
Berkeley, California 94720

ABSTRACT

This paper presents a conceptual and numerical model of multiphase flow in fractures. The void space of real rough-walled rock fractures is conceptualized as a two-dimensional heterogeneous porous medium, characterized by aperture as a function of position in the fracture plane. Portions of a fracture are occupied by wetting and non-wetting phase, respectively, according to local capillary pressure and accessibility criteria. Phase occupancy and permeability are derived by assuming a parallel-plate approximation for suitably small subregions in the fracture plane. For log-normal aperture distributions, a simple approximation to fracture capillary pressure is obtained in closed form; it is found to resemble the typical shape of Leverett's j-function. Wetting and non-wetting phase relative permeabilities are calculated by numerically simulating single phase flows separately in the wetted and non-wetted pore spaces. Illustrative examples indicate that relative permeabilities depend sensitively on the nature and range of spatial correlation between apertures. It is also observed that interference between fluid phases flowing in a fracture tends to be strong, with the sum of wetting and non-wetting phase relative permeabilities being considerably less than 1 at intermediate saturations.

INTRODUCTION

Fluid flow in geologic media is often dominated by the highly permeable pathways provided by rock fractures and joints. Multiphase flow through fractures occurs in many subsurface flow systems that are of engineering interest in the context of energy resource recovery (petroleum, natural gas, geothermal water and steam) and environmental protection (chemical and radiation contamination in groundwater aquifers, partially saturated zones). It also plays a crucial role in petroleum migration and ore deposition, and in the evolution of hydrothermal convection systems.

From a practical viewpoint, the most important example of multiphase flow is in petroleum reservoirs, many of which are situated in fractured-porous formations (Weber and Bakker, 1981). In these reservoirs, two- and three-phase flow of oil, water, and gas occurs naturally and in response to production and injection operations. Many natural gas reservoirs with two-phase flow of gas and water are located in tight rocks with predominant fracture permeability. A different kind of two-phase flow, namely, water/vapor flow with strong phase change and latent heat effects, occurs in geothermal reservoirs and in hydrothermal convection systems. Most of these systems are found in fractured rocks with low matrix permeability (typically of order $10^{-18} m^2 = 1$ microdarcy). Strong two-phase flow effects of water/vapor and water/noncondensible gas are expected near geologic repositories for heat-generating or corroding radioactive wastes (Pruess, 1989).

In the analysis of multiphase flows it is important to carefully distinguish between fluid phases and components. Phases are the "physical" and components the "chemical" building blocks of a fluid system. Throughout a fluid phase, thermophysical properties such as pressure, temperature, and viscosity vary continuously and smoothly from point to point, while these properties will undergo discontinuous jumps at phase boundaries. The surface tension effects at the interface between fluid phases give rise to capillary pressure phenomena. Fluid components distribute themselves among phases according to solubility and volatility. For example, in a high-pressure mixture of water, a heavy hydrocarbon

and CO_2, most of the CO_2 may reside in a dense gas-like phase, while a large amount would be dissolved in the oil phase, and a smaller amount in the aqueous phase.

The behavior of a two-phase system may be rather different, depending on whether it consists of a single component, such as liquid water/water vapor, or two or more components, such as water and oil, or water and a non-condensible gas. For example, a gas phase can evolve inside a body of liquid water by phase transformation (boiling) in response to suitable changes in temperature and pressure. The gas (vapor) phase need not be topologically connected to a contiguous body of vapor. This is in contrast to two-component two-phase systems, where the phase composition in a region can only change if an invading phase can access the region through a continuous flow path. Thus, for single component two-phase systems the pore space occupancy depends only on a local "allowability" criterion, which determines whether for given capillary suction conditions a certain portion of the pore space will be occupied by wetting or non-wetting phase. For two-component systems, an additional global "accessibility" criterion needs to be satisfied, which determines whether or not a fluid phase can in fact reach an allowed pore segment. In addition to phase occupancy, there are also differences in phase mobilities between single- and multicomponent systems. Through a thermodynamic analysis, Verma (1986) showed that in single-component systems vapor bubbles cannot get trapped at liquid-filled pore throats in concurrent vapor-liquid flow, while under suitable capillary pressure conditions the non-wetting phase in a two-component systems may get trapped.

When several fluid phases are present simultaneously in the void space of a porous medium, or in a rock fracture, the presence of any one of the phases will interfere with the flow of all the others. Quantitatively, this permeability reduction is expressed in terms of relative permeability factors k_r, so that for a medium with absolute (intrinsic) permeability k, the effective permeability to a fluid phase β (= aqueous, gas, oil, ...) is given by $k \cdot k_{r,\beta}$. The relative permeability functions vary between 0 and 1, where $k_{r,\beta} = 0$ corresponds to very strong phase interference with phase β completely immobile

because of the presence of other phases, and $k_{r,\beta} = 1$ corresponds to negligible phase interference, i.e., essentially single-phase flow of phase β. Experimental and theoretical work has established that the relative permeability functions are primarily dependent on the void space fraction or "saturation" S_β occupied by a fluid phase (Scheidegger, 1974). More complicated effects, including dependence on capillary number and saturation history (hysteresis), are also well documented (Fulcher et al., 1985; Honarpour et al., 1986).

PREVIOUS WORK AND A NEW APPROACH

The relative permeability functions are of fundamental importance in the analysis of multiphase flows, because they determine the ease with which any fluid phase can flow in the presence of other phases. It is generally accepted that over a wide range of conditions multiphase flows in porous media can be described with an extension of Darcy's law, as follows (Scheidegger, 1974; Peaceman, 1977):

$$\underset{\sim}{F}_\beta = -k \frac{k_{r,\beta}}{\mu_\beta} \rho_\beta (\nabla P_\beta - \rho_\beta \underset{\sim}{g}) \tag{1}$$

where $\underset{\sim}{F}_\beta$ is the mass flux in phase β, k is absolute (intrinsic) permeability, $k_{r,\beta}$ is relative permeability, μ_β is viscosity of fluid phase β, ρ_β is fluid density, P_β is pressure in phase β, and $\underset{\sim}{g}$ is acceleration of gravity. A number of experiments have been reported (summarized by Scheidegger, 1974), which show that Eq. (1) is a satisfactory approximation for describing multiphase flow in porous media. Given the wide occurrence and practical importance of multiphase flow in fractures, it is surprising that very little quantitative information on such flows is available. Experimental work undertaken in connection with compressed gas storage in mined rock caverns has demonstrated multiphase flow effects in fractures (Barton, 1972; Bawden and Roegiers, 1985). Merrill (1975) performed two-phase flow experiments in artificial fractures, but he was unable to correlate experimental flow data by means of relative permeability functions. The only published experimental data on fracture relative permeabilities that we are aware of are those of Romm (1966), who observed two-phase flow of water and kerosene in artificial parallel-plate fractures, which were lined with strips and sheets of celluloid or polyethylene film

and waxed paper. Romm obtained a linear dependence of relative permeability on saturation for the entire range of $0 < k_r < 1$, with $k_{r,w} = S_w$, $k_{r,nw} = S_{nw}$, so that $k_{r,w} + k_{r,nw} = 1$. For lack of other data Romm's relative permeabilities have been widely used in numerical simulations of fractured petroleum reservoirs (e.g., Gilman and Kazemi, 1983), although it appears unlikely that Romm's results would be applicable to relative permeabilities of real rough-walled rock fractures.

The lack of laboratory data is probably due to difficulties in controlling and measuring phase saturations in fractures. Standard laboratory techniques such as gamma ray or microwave attenuation devices are sensitive to the volumetric composition of a multi-phase system. The void volumes present in fractures, however, are invariably small compared to sample volumes and interstitial voids in unfractured material, so that the application of volumetric methods meets with great difficulties and inaccuracies.

Possibilities for obtaining relative permeability information from field data on multiphase flows are also limited, because it is all but impossible to simultaneously measure flow rates, pressure gradients, and phase saturations in the subsurface. An approximate analysis can be made for geothermal wells with two-phase steam/water flow. Based on observed correlations between flowrate and flowing enthalpy for a number of wells in the fracture-dominated Wairakei geothermal field, Grant (1977) concluded that relative permeabilities tend to be larger than generally accepted for porous media. Using an extension of Grant's method, Pruess et al. (1983, 1984) and Bodvarsson et al. (1987) analyzed production data from the fracture-dominated geothermal fields at Krafla, Iceland, and Olkaria, Kenya. Their analysis indicated that the sum of liquid and vapor relative permeabilities remained close to 1 for the entire range of flowing enthalpies, from pure liquid throughout the two-phase region to pure vapor flow. These results are consistent with Romm's findings, although the dependence of relative permeabilities on phase saturations could not be determined from the field data. However, this consistency with Romm appears fortuitous. As will be discussed below, the near-constancy of the sum of liquid and vapor relative permeabilities over a wide range of flow conditions most likely

reflects phase transformation effects specific to a single-component two-phase system. The results obtained in this paper indicate that at intermediate saturations the relative permeabilities of rough-walled fractures will generally be smaller than those for media with intergranular porosity.

From a theoretical viewpoint the subject of multiphase flow in fractures has also received very little attention. The chief obstacle here seems to be that until recently there was a lack of credible models for the pore space geometry in natural rock fractures. Evans and coworkers have used capillary theory to study the multiphase flow behavior of systems of idealized parallel-plate fractures (Evans, 1983; Evans and Huang, 1983; Rasmussen et al., 1985), and of wedge-shaped fractures with continuously varying apertures (Rasmussen, 1987). Newly developed imaging techniques (Gentier, 1986; Pyrak-Nolte et al., 1987; Hakami, 1988) have led to the conceptualization of fractures as two-dimensional heterogeneous porous media, with flow taking place in intersecting channels of varying aperture (Tsang and Tsang, 1987; Wang et al., 1988; Montazer et al., 1988). These emerging concepts open the way for new theoretical approaches to multiphase flow in fractures.

The approach developed in this paper for predicting two-phase relative permeability in fractures is based on the conceptualization of rough-walled rock fractures as two-dimensional porous media, whose void space can be characterized by specifying the aperture as a function of position. We introduce the hypothesis that, as far as multiphase flow properties are concerned, a rough-walled fracture with position-dependent aperture behaves locally like a parallel-plate fracture with the same average aperture. This is clearly an approximation which requires experimental confirmation. The approximation is expected to be applicable under conditions where the distance over which fracture apertures are correlated is large compared to the apertures themselves. The local parallel-plate approximation allows to predict phase occupancy and permeability for any suitably small subregion of the fracture plane. The global relative permeability behavior of a rock fracture is then obtained by discretizing the fracture into a large number of

connected parallel plates of different apertures. Numerical simulation is used to synthesize multiphase flow on a larger scale from the known phase occupancy and permeability characteristics of the individual parallel-plate segments.

The main emphasis in the present work is on the development of a new approach for predicting fracture relative permeabilities from an assumed or known void space geometry. The approach is illustrated by application to fracture geometries that are generated by stochastic methods on a computer, using experimentally-based aperture distribution and spatial correlation properties. Although schematic in nature, the applications reveal some interesting characteristics of fracture relative permeabilities, including the generally strong nature of phase interference effects, and the crucial role of long-range spatial correlations among apertures. Our approach is also applicable to actual experimental "images" of fracture void geometry, as obtained by means of casting techniques (Gentier, 1986; Pyrak-Nolte et al., 1987), or spectroscopic-tomographic methods.

TWO–DIMENSIONAL POROUS MEDIA

In the hydrologic literature fractures have often been idealized as the void space enclosed between two parallel plates (de Marsily, 1986). "Real" rock fractures, however, have rough surfaces with numerous contact points. Recent observations indicate that the topography of fracture walls may have fractal structure (Brown and Scholz, 1985; Wang et al., 1988). In this paper we focus on "small" fractures in hard rock, with apertures typically in the submillimeter range, as opposed to fracture zones which consist of a layer of highly permeable material sandwiched between rock of low permeability. Fracture zones may have widths of order 0.1 to 1 m and have a three-dimensional pore structure. In contrast, the small fractures considered here consist of the void space enclosed between two impermeable surfaces, which in a topological sense constitutes a two-dimensional porous medium. Quantitatively this can be described by specifying the two fracture surfaces, $z_i = z_i(x,y)$ for $i = 1, 2$. Alternatively, one can specify the midplane $z = (z_1 + z_2)/2$ and the local aperture $b(x,y) = z_2 - z_1$. For simplicity we assume fractures to be planar in the following ($z = $ const.); however, this assumption is made only for

convenience and is not necessary for our model. The important property of the fracture model developed here is the two-dimensional nature of the pore space.

Several different techniques have been used to experimentally characterize apertures of rough-walled fractures, including linear profilometer scans (e.g. Brown and Scholz, 1985; Gentier, 1986), two-dimensional imaging from replicas of the pore space made by injection of Woods' metal or epoxy resins (Pyrak-Nolte et al., 1987; Gale, 1987; Gentier et al., 1989), and application of fluid drops of known volume (Hakami, 1988). Different scales of spatial correlation among apertures have been noted experimentally (Gentier, 1986). In various instances fracture apertures have been found to follow a skewed distribution well approximated by a log-normal distribution (Gentier, 1986; Gale, 1987; Hakami, 1988). The log-normal distribution is given by the following expression (aperture $b \geq 0$)

$$n(b) = \frac{1}{\sqrt{2\pi}\,(\sigma \ln 10)}\, \frac{1}{b}\, \exp\left(\frac{-[\log b - \log b_o]^2}{2\sigma^2}\right) \tag{2},$$

where b_o is the most probable aperture, and σ the variance. The corresponding mean aperture $\bar{b}$ is larger than the most probable aperture; it is

$$\bar{b} = b_o \exp\left(\frac{(\sigma \ln 10)^2}{2}\right) \tag{3}$$

Figure 1 shows a log-normal distribution with a mean aperture $\bar{b} = 81.8\ \mu m$ and a variance of $\sigma = 0.43$ (most probable aperture $b_o = 50\mu m$). Note that the log-normal distribution is strongly biased towards small apertures. Most apertures are considerably smaller than the mean aperture, while there is a small proportion of relatively large apertures.

SPATIAL CORRELATION AND DISCRETIZATION OF APERTURES

In addition to the aperture distribution, a crucial aspect of fracture apertures is that they are spatially correlated, generally in anisotropic fashion, over some distance in the fracture plane. In the present study, we use geostatistical methods to generate discretized aperture distributions in the fracture plane. In most cases we use a lognormal distribution

of apertures with an exponential spatial covariance. The aperture generation code COVAR (William and El-Kadi, 1986) was modified to allow for anisotropic covariance. The input parameters to the aperture generation code are $\log b_o$, σ, λ_x, and λ_y, which denote, respectively, the mean and standard deviation of the lognormal distribution, and the spatial correlation lengths in x and y directions.

Figures 2 and 3 show stochastic realizations of lognormal aperture distributions in a fracture plane with different length and anisotropy of spatial correlation. The parameters for these distributions are given in Table 1.

Adopting a finite spatial resolution $\Delta x \times \Delta y$ results in a discretized representation of fracture apertures, with average aperture being b_{ij} in the element $(x_i - \Delta x/2, x_i + \Delta x/2; y_j - \Delta y/2, y_j + \Delta y/2)$ of the fracture plane. In the calculations reported below we use a 20×20 grid to discretize a $40mm \times 40mm$ portion of a fracture plane, so that $\Delta x = \Delta y = 2mm$. Figures 4 and 5 show discretized counterparts of the aperture distributions given in Figures 2 and 3. For convenience, we will use a shorthand notation (i,j) for an element of the fracture plane. Although, in this paper, discretized representations of fracture apertures were generated from continuous distributions through stochastic techniques, such representation can also be directly obtained from laboratory specimen by digitizing pore space images into a finite number of "pixels".

RELATIVE PERMEABILITY MODEL

It is well established that for single-phase flow the permeability of a parallel-plate fracture of aperture b is given by (de Marsily, 1986)

$$k = \frac{b^2}{12} \tag{4}$$

This permeability is present over a flow sheet of width b so that, when normalized to a unit thickness perpendicular to the fracture, the average permeability is

$$\bar{k} = \frac{b^3}{12} \tag{5}$$

whence the term "cubic law" for this relationship. In two-phase conditions, the capillary pressure between wetting and non-wetting phases is given by

$$P_c = \frac{2\gamma \cdot \cos \alpha}{b} \tag{6}$$

where γ is the surface tension between wetting and non-wetting phases, and α is the contact angle between the wetting phase meniscus and the fracture wall. We adopt the convention of taking $P_c > 0$, and we assume that the contact angle for water-vapor (or wetting-nonwetting phase) is 0.

The crucial concept developed in this paper can now be stated as follows: As far as multiphase flow properties are concerned, a rough-walled fracture with position-dependent aperture is assumed to behave locally like a parallel-plate fracture with the same average aperture (Brown, 1987; Pyrak-Nolte et al., 1988). Thus, a fracture element with aperture b_{ij} has a single-phase permeability $b_{ij}^2/12$, and its phase occupancy is governed by the local capillary pressure $P_{ij} = 2\gamma/b_{ij}$. In "quasistatic" conditions of low pressure gradients. (low capillary number), when both wetting and non-wetting phase have access to the fracture element (i,j), the phase "allowability" will be as follows. For an externally imposed capillary suction pressure P_c, the fracture segment (i,j) will contain wetting phase if $P_c < P_{ij}$, non-wetting phase if $P_c > P_{ij}$. Note that this assumption ignores possible effects from wetting phase which may be held by small-scale roughness or by adsorptive forces in the walls of fracture elements the bulk of which would be drained (Pruess et al., 1988). Mineral coatings may also play a role in complicating phase occupancy and mobility (N.G.W. Cook, private communication).

Our procedure for calculating capillary pressures and relative permeabilities is as follows.

(1) Obtain a discretized representation b_{ij} of fracture apertures for a finite rectangular domain, either by generating a stochastic realization of a suitable aperture distribution, or by directly digitizing an image of the pore space (see Figures 4 and 5).

(2) Define a cutoff-aperture b_c, corresponding to a capillary pressure $P_c = 2\gamma/b_c$, and occupy all accessible apertures smaller than b_c with wetting phase, all larger apertures with non-wetting phase. Calculate the saturation S_w (and $S_{nw} = 1 - S_w$) corresponding to the cutoff capillary pressure P_c by directly summing the wetted pore volume.

(3) Apply suitable constant-pressure conditions at the boundaries of the fracture, and simulate fluid flow in the network of occupied fracture elements. (In our simulations, flow is taking place in the x-direction, with no-flow boundaries at $y = 0$ and $y = 1$; see Figures 4 and 5.) The steady-state flow rate obtained when only apertures less than b_c are occupied will yield the effective wetting phase permeability; a similar simulation with only apertures larger than b_c occupied will yield the effective non-wetting phase permeability. It should be noted that it is only under conditions of small capillary number that the two-phase flow problem in the fracture plane separates into two single-phase flow problems. When sizeable pressure gradients are present the flowing phases will be able to invade otherwise "forbidden" pores.

(4) Division of the effective phase permeability by the single-phase permeability (all apertures occupied) yields the relative permeability at saturation S_w. Repeat the procedure for a range of b_c (and S_w) to obtain the entire relative permeability and capillary pressure curves.

NUMERICAL SIMULATIONS

In order to implement the procedure outlined above it is necessary to derive the transmissivity between fracture elements of different aperture. Consider a "connection" (flow contact) between two fracture elements with apertures b_n and b_m, respectively (Figure 6). Neglecting non-linear flow effects at the juncture, the total pressure drop between n and m can be expressed as

$$P_n - P_m = (P_n - P_i) + (P_i - P_m)$$
$$= F_{mn} \frac{\mu}{\rho} \left\{ \frac{D_n}{k_n A_n} + \frac{D_m}{k_m A_m} \right\} \qquad (7)$$

Here P_i denotes the pressure at the interface, F_{mn} is the mass flow rate, μ is fluid viscosity, ρ is density, and D_n, k_n, A_n are nodal distance, permeability, and cross-sectional area for flow in fracture element n, respectively (likewise for element m). Introducing an effective permeability k_{mn} and connection area A_{mn}, the pressure drop can also be written as

$$P_n - P_m = F_{mn} \frac{\mu}{\rho} \frac{D_n + D_m}{k_{mn} A_{mn}} \qquad (8)$$

Equating the expressions (7) and (8), and inserting for flow area $A_n = b_n \times \Delta y$, similarly for A_m, and using Eq. (4) for permeability, we obtain

$$k_{mn} A_{mn} = \frac{(D_n + D_m) \Delta y}{12 \left[\dfrac{D_n}{b_n^3} + \dfrac{D_m}{b_m^3} \right]} \qquad (9)$$

indicating that only the product of effective interface permeability k_{mn} and interface area A_{mn} is defined. For the numerical implementation we find it convenient to take $k_{mn} = k$ = const. for all flow connections. With this convention we obtain

$$A_{mn} = \frac{(D_n + D_{m)} \Delta y}{12k \left[\dfrac{D_n}{b_n^3} + \dfrac{D_m}{b_m^3} \right]} \qquad (10)$$

for "active" (occupied) connections; $A_{mn} = 0$ for inactive connections.

We have incorporated these equations into our general-purpose simulator "MULKOM" (Pruess, 1983, 1988), which solves discretized mass and heat balance equations for multiphase flows in porous media. The version of MULKOM used in the present work describes single-phase isothermal flow of an incompressible fluid with constant viscosity.

For numerical simulation the continuous space and time variables must be discretized. In MULKOM space discretization is made directly from the integral form of the basic conservation equations, without converting them into partial differential equations. This "integral finite difference" method (Narasimhan and Witherspoon, 1976) avoids any reference to a global system of coordinates, and thus offers the advantage of being applicable to regular or irregular discretizations in one, two, or three dimensions. Time is discretized fully implicitly as a first-order backward finite difference. This together with 100% upstream weighting of flux terms at interfaces is necessary to achieve unconditional stability (Peaceman, 1977), and to avoid impractical time step limitations when simulating flow in regions with small grid blocks. The discretization results in a set of strongly coupled nonlinear algebraic equations, which are solved completely simultaneously, using Newton-Raphson iteration. Time steps are automatically adjusted (increased or reduced) during a simulation, depending on the convergence of the iteration process. The linear equations arising at each iteration step are solved with a sparse version of LU-decomposition and backsubstitution (Duff, 1977).

Minor code changes were made to improve the calculational efficiency for small fracture domains, in which individual fracture elements, represented as separate grid blocks, have small linear dimensions of order 1 mm. A fictitious very large fluid viscosity (of order 10^6 Pa·s) was specified to scale up pressure differences between neighboring grid blocks and thereby diminish numerical cancellation errors. Automatic adjustment of time steps and convergence criteria was used to expedite and recognize attainment of a steady state.

From the numerical simulation we obtain, for any given aperture cutoff b_c, the total steady-state flow rate $F(b_c)$ across the fracture between boundaries separated by a distance L and held at a pressure difference of ΔP. A straightforward application of Darcy's law gives the following expression for effective permeability for aperture cutoff b_c:

$$k(b_c) = \frac{F(b_c)}{A} \frac{\mu}{\rho} \frac{L}{\Delta P} \tag{11}$$

The permeability in Eq. (11) is normalized to a cross-sectional area A, which we take to

be $1\,m^2$; i.e., it is assumed that the modeled fracture segment is embedded in a cross-sectional area of $1 \times 1\,m^2$. Defining k_o as the permeability obtained when all apertures are occupied, the relative permeability for an aperture cutoff b_c, corresponding to a saturation S_w, is obtained by

$$k_r(b_c) = \frac{k(b_c)}{k_o} \tag{12}$$

Actually, two values are obtained, namely, a relative permeability for the wetting phase where all apertures $b < b_c$ are occupied, and one for the non-wetting phase with occupancy in the apertures with $b > b_c$.

RESULTS AND DISCUSSION

Capillary Pressure

In the first illustrative calculations presented here we have ignored issues of pore accessibility, which amounts to neglecting hysteresis effects. Pore occupancy is determined solely based on the capillary allowability criterion; i.e., for an externally applied capillary pressure $P_c = 2\gamma/b_c$, all apertures $b < b_c$ are assumed to contain wetting phase, all apertures $b > b_c$ contain non-wetting phase. Wetting phase saturation is then simply given by the fractional pore volume with apertures $b < b_c$, which for the log-normal distribution Eq. (2) can be explicitly evaluated in closed form (see appendix); the result is

$$S_w = \frac{1}{2}\,\text{erfc}\left[\frac{\log b_o/b_c + \sigma^2 \ln 10}{\sqrt{2\sigma^2}}\right] \tag{13}$$

where "erfc" denotes the customary complementary error function (Carslaw and Jaeger, 1959; Abramowitz and Stegun, 1965). Introducing the capillary pressure $P_{c,o}$ corresponding to the most probable aperture b_o, $P_{c,o} = 2\gamma/b_o$, Eq. (13) can be explicitly rewritten as a capillary pressure-saturation relationship by substituting b_o/b_c with $P_c/P_{c,o}$. A plot of Eq. (13) for $b_o = 50\mu m$ ($\bar{b} = 81.8\mu m$) is given in Figure 7 (curve labeled "analytical").

The general appearance of the capillary pressure curve is similar to the customary j-function (Leverett, 1941) for three-dimensional porous media. Most of the wetting phase saturation range is traversed for inverse apertures from 10^3 to $10^4\,\mathrm{m}^{-1}$, which for a water/air system with surface tension of approximately 0.072 N/m at ambient temperature corresponds to rather weak capillary pressures from 144 to 1440 Pa. These values pertain to a fracture with a relatively large average aperture of 81.8 μm, and, for a fracture with different average aperture, would scale inversely proportional to the aperture. Smaller fractures with apertures in the range of a few μm will exert stronger capillary pressures in the range of a few bars (1 bar $\equiv 10^5$ Pa), as has been observed in recent experimental studies (Firoozabadi and Hauge, 1989).

Note that the capillary pressure-saturation relationship Eq. (13) depends only on the variance σ of the log-normal distribution and the ratio b_o/b_c of the most probable aperture b_o to the cutoff aperture b_c. Thus, the relationship between capillary pressure and saturation for fractures with lognormal aperture distribution of fixed variance σ has the same functional form, regardless of the magnitude of the most probable aperture b_o. When all apertures are scaled by a common factor, capillary pressure at a given saturation will scale by the inverse of that factor.

It should be noted that the simple concept leading to Eq. (13) has several limitations, so that the result should only be considered a first approximation. First of all, the phase occupancy rule neglects effects of pore space accessibility. Portions of the fracture plane are occupied solely on the basis of a local capillary allowability criterion, so that hysteresis effects from different pore accessibilities during drying and wetting cycles are ignored. Secondly, implicit in the capillary allowability criterion is the assumption that the fracture behaves like a parallel plate locally.

Effects from global accessibility can be easily taken into account by considering spatially discretized realizations of continuous aperture distributions. This approach has been used by Tsang and Hale (1988) to simulate hysteretic capillary pressure curves for

rough-walled fractures.

The local parallel-plate approximation will be applicable under conditions when fracture apertures are correlated over spatial distances that are larger than the apertures themselves. This may not be satisfied for fractures with very rough walls.

In spite of these limitations, the capillary pressure relationship Eq. (13) is attractive because of its simplicity and intuitive appeal.

The curve labeled "random" in Figure 7 shows the capillary pressure curve corresponding to the 400 computer-generated lognormally distributed apertures, that were used as a basis for numerical simulation of flow in fractures discretized into 20 x 20 parallel plate segments. This curve agrees generally very well with the exact analytical result. Some discrepancies are apparent at the weakest capillary pressures, corresponding to the largest fracture apertures. This is due to the poor statistics of the small number of large apertures present in a sample of only 400 apertures. The curve labeled "correlated" represents the capillary pressures corresponding to the spatially correlated counterpart (with $\lambda_x = \lambda_y = 0.2$) of the 400 random data. This curve should coincide with the "random" curve, but some systematic deviations are apparent. For strong capillary pressures, wetting phase saturations are somewhat too low; agreement is rather good at intermediate saturations, while at weak capillary pressures wetting saturation is too large. This trend was apparent in all of our numerical experiments, indicating that in the spatial correlation process executed in the COVAR program (William and El-Kadi, 1986), apertures were biased somewhat away from the small and large limits towards the most probable aperture range.

Relative Permeability

We verified the accuracy of the numerical simulation procedure for obtaining steady-state flows by comparison with computations using an electric resistor analog. Simulations were then performed for a number of discretized realizations of lognormal and

normal aperture distributions with different mean values and spatial correlation lengths. Figures 8 and 9 show results for wetting and nonwetting phase relative permeabilities, respectively, for the two aperture distributions of Figures 4 and 5 (parameters as given in Table 1). The different data points in Figures 8 and 9 correspond to different cutoff apertures b_c.

Before discussing the simulation results presented in Figures 8 and 9 it should be emphasized that these are to be considered a first rough illustration of the trends; due to various approximations and idealizations involved they are not expected to provide a quantitatively valid evaluation of fracture relative permeabilities. The test calculations performed so far indicate that relative permeability predictions depend sensitively on the details of spatial correlation between apertures; a realistic description of these correlations is required before quantitatively useful results can be obtained. Other limitations arise from the stochastic nature of the aperture distributions; calculations for a reasonably large number of realizations would be needed before firm conclusions can be drawn. The rather coarse discretization (20×20) of the fracture plane and the five-point finite difference scheme used here result in spatial discretization errors (Forsythe and Wasow, 1960; Yanosik and McCracken, 1979). By restricting flow connections to the four nearest neighbors with a shared interface, the five-point scheme will produce an overestimate of flow interference between phases.

The most remarkable feature of the relative permeability curves shown in Figure 8 is the apparent strong interference between the phases: Immobile nonwetting phase saturation is extremely large, about 84%, and a saturation "window" in which both phases would be mobile is virtually non-existent. This contrasts with the behavior shown in Figure 9, where immobile nonwetting saturation is a more modest (although still large) 51.5%, and there is a considerable range of saturations over which both phases can flow simultaneously. In our calculations so far we have generally found that a significant window of two-phase mobility exists only for anisotropic aperture distributions, with considerably larger spatial correlation length in the direction of flow than perpendicular to it.

Our wetting phase relative permeabilities appear to be generally similar to experimental results for (three-dimensional) porous media (Osoba et al., 1951; Corey, 1954; Johnson et al., 1959; Brooks and Corey, 1964), while non-wetting phase relative permeabilities are predicted to drop off rather rapidly with increasing wetting phase saturation.

This can be understood from the characteristics of the lognormal distribution, in which there are many relatively small apertures and a small number of large apertures. If there are no long-range spatial correlations between apertures (see Figure 2), a contiguous flow path for nonwetting phase can only be maintained when in addition to all the large apertures also some of the smaller apertures contain nonwetting phase. In other words, a relatively large nonwetting phase saturation is required before nonwetting phase can flow.

Phase interference is generally stronger in two-dimensional than in three-dimensional porous media, because there are fewer alternative routes for bypassing inaccessible pores. (In percolation theory parlance, two-dimensional media have a smaller coordination number; Heiba et al., 1982). Anisotropic spatial correlation, with larger correlation length in the direction of flow, tends to segregate the small aperture and the large aperture pathways (see Figure 3). This diminishes phase interference and broadens the saturation window for two-phase mobility (Figure 9). The sudden jump in non-wetting phase relative permeability at $S_w = 48.5\%$ occurs because of a single pore throat located near $x = 0.5$, $y = 0.3$ (see Figures 3 and 5).

At the present time there are no reliable observational data with which our predictions for fracture relative permeabilities can be compared. However, as had been mentioned above, there is some evidence from fractured geothermal reservoirs which suggests that the sum of liquid and vapor relative permeabilities is close to 1 over the entire range of saturations (Grant, 1977; Pruess et al., 1983, 1984; Bodvarsson et al., 1987). Such behavior is not necessarily in disagreement with our findings; in fact, it is straightforward to identify geometric characteristics of fracture aperture distributions that would lessen

or completely eliminate interference between phases, and thereby give rise to larger wetting and nonwetting phase relative permeabilities at intermediate saturations.

For example, it is quite conceivable that fractures commonly have certain long-range spatial correlations between apertures. These could be provided by channels or rivulets formed by mechanical erosion or mineral dissolution processes. Another possibility is that field-determined relative permeabilities could pertain to an aggregate response of several fractures of different magnitude, with wetting phase flowing in the smaller fractures, nonwetting phase in the larger ones. Under such conditions of segregated flow the sum of wetting and nonwetting phase relative permeabilities would be near 1 at all levels of saturation.

In addition to geometric characteristics of the fracture pore space, there is a purely thermodynamic effect that will enhance nonwetting phase permeability in single-component two-phase flow. As was shown by Verma (1986), phase transformation effects will prevent vapor bubbles from getting trapped at pore throats in concurrent vapor-liquid flow. Verma's analysis indicates that phase change processes will in effect enable vapor flow to take place even if there is no contiguous flow path for the vapor phase. This effect would generally enhance nonwetting phase relative permeability in single-component two-phase systems (a volatile fluid and its vapor) in comparison to two-component systems. We suggest that this flow enhancement mediated by phase change is the most likely explanation for the observation that $k_{rl} + k_{rv} \approx 1$ in geothermal reservoirs.

Our model for two-phase fracture relative permeabilities does not include phase change effects, so that our predictions should be more relevant for two-component systems such as oil-water or water-gas.

CONCLUDING REMARKS

We have developed a new conceptual approach for predicting wetting and nonwetting phase relative permeabilities in real rough-walled rock fractures. Our method utilizes a quantitative description of the fracture pore space in terms of an aperture distribution, which can be obtained either through direct laboratory measurements on fracture specimens, or by means of stochastic computer-generated realizations of mathematical distribution functions. The crucial concept used in our method is that the capillary and permeability properties of a fracture can be approximated by a parallel-plate model locally. This is a hypothesis which requires further experimental and theoretical study.

First applications of the method involved computer simulation of flow in fractures with synthetic (lognormal) aperture distributions. It was found that interference between phases is generally strong. The sum of wetting and nonwetting phase relative permeabilities is much less than 1 at intermediate saturations, unless there are long-range spatial correlations among apertures in the direction of flow. Such correlations are likely to occur commonly in fractures in the form of channels or rivulets. Even so, first results seem to indicate that immobile non-wetting phase saturations in fractures may be large, of order 50%. However, this result may only be applicable to two-component two-phase systems, such as water and gas (or air), or water and oil. In geothermal reservoirs we are dealing with essentially single-component (water) two-phase systems. In these systems phase change provides an additional degree of freedom in two-phase flow, which will diminish or eliminate blocking of one phase by the other, and thereby enhance nonwetting phase relative permeability.

There is some evidence from fractured geothermal reservoirs that the sum of liquid and vapor relative permeabilities is close to 1 at all saturations. We suggest that this feature is most likely due to the indicated phase transformation effects rather than due to peculiar features of fracture as opposed to porous medium flow, as has often been assumed in the geothermal literature. All else being equal, the sum of wetting and nonwetting phase relative permeabilities at intermediate saturations should be smaller in fractures than in

three-dimensional porous media, because of the reduced possibility for bypassing inaccessible pores.

Relative permeability behavior will become more complicated for larger capillary numbers, where sufficient pressure drive may be present to permit a phase to invade pore spaces that would not be allowed based on a static criterion of local capillary pressure. We expect effects of flow interference and blocking of phases to diminish with increasing capillary number, so that relative permeabilities at intermediate saturations and especially near the irreducible limits would be larger than predicted from a capillary allowability criterion. Indeed, laboratory flow experiments in porous media have established that residual non-wetting phase saturation decreases as wetting phase flow rate increases (Abrams, 1975; Labastie et al., 1980). Similar effects would also arise when flow through the rock matrix or the possibility of wetting phase flow along the fracture walls are taken into account. Matrix and wall flow could provide mechanisms for bypassing unallowed pores in the fracture plane.

The illustrative calculations presented in this paper have neglected effects of accessibility of non-uniform apertures in the fracture plane. Such effects will enhance the wetting and diminish the non-wetting phase saturation and relative permeability during drainage. The opposite effects from accessibility (enhanced non-wetting and diminished wetting phase saturation and relative permeability) are expected for the imbibition cycle.

Predictions of fracture relative permeabilities from void space geometry obviously can not be more realistic than the aperture distributions on which they are based. Our numerical experiments have used rather schematic, idealized distributions, and the results presented in Figures 8 and 9 are to be viewed as a first illustration of trends. Even so, we believe that some important conclusions can be drawn. It appears that, as far as two-phase flow properties are concerned, the most crucial aspect of fracture void space geometry is the presence or absence of long-range correlations among apertures. Under mixed-phase occupancy and for small capillary numbers (capillary forces dominating

over viscous drag), non-wetting phase can only flow in a fracture plane if there are throughgoing pathways that avoid the small apertures which would be blocked by wetting phase. This requires long-range spatial correlations among the "large" apertures. Similarly, throughgoing pathways for wetting phase will only be available if there are pathways than can avoid "large" apertures, requiring long-range correlations among "small" apertures. In fractures with lognormal aperture distributions, the "irreducible" wetting phase saturation (smallest saturation at which wetting phase can flow) will generally be considerably smaller than the irreducible non-wetting phase saturation, due to the preponderance of small apertures. Determination of the saturation conditions under which liquid (aqueous) phase flow can take place in fractures is of crucial importance for evaluating the suitability of the proposed high-level nuclear waste repository site at Yucca Mountain, Nevada.

It appears likely that the relative permeability behavior of different kinds of fractures may be quite different. Our numerical experiments suggest that the single most important feature affecting multiphase flow in "small" fractures in tight rocks is the long-range spatial correlations among fracture apertures. Experimental work in the laboratory and in the field is needed to quantify fracture void space geometry, with special emphasis on identifying the extent and nature of spatial correlations among fracture apertures.

NOMENCLATURE

A	area, m^2
b	fracture aperture, m
b_c	cutoff aperture, m
b_o	most probable aperture, m
$\bar{b}$	mean aperture (Eq. 3), m
D	distance between finite-difference nodes, m

erf	error function, dimensionless
erfc	complementary error function, dimensionless
$\underset{\sim}{F}$	mass flux, $kg/m^2 \cdot s$
$\underset{\sim}{g}$	acceleration of gravity, m^2/s
k	(intrinsic) permeability, m^2
k_o	(intrinsic) fracture permeability for single-phase flow, m^2
k_r	relative permeability, dimensionless
ln	natural logarithm, dimensionless
log	logarithm to base 10, dimensionless
L	length of fracture between constant-pressure boundaries, m
n	frequency distribution of fracture apertures (Eq. 2), dimensionless
$\tilde{n}$	normal distribution (appendix), dimensionless
P	pressure, Pa
P_c	capillary pressure, Pa
S	saturation (volume fraction of a fluid phase), dimensionless
S_w	saturation of wetting phase, dimensionless
S_{nw}	saturation of non-wetting phase, dimensionless
u	logorithm (to base 10) of fracture aperture, dimensionless
v	$= \sigma^2 \ln 10 + \log b_o$ (appendix), dimensionless
x	coordinate in flow direction in fracture plane, m
y	coordinate perpendicular to flow direction in fracture plane, m
z	elevation of fracture surface

Greek

α	contact angle, radians

γ	interfacial tension, N/m
λ	spatial correlation length of fracture apertures, m
σ	variance of fracture aperture distribution, dimensionless
μ	viscosity, Pa $\cdot$ s
ρ	density, kg/m^3

Subscripts

c	capillary
i, j, n, m	finite difference grid blocks
l	liquid
nw	non-wetting
r	relative
v	vapor
w	wetting
β	fluid phase (β = w: wetting, nw: non-wetting)

ACKNOWLEDGEMENT

REFERENCES

Abramowitz, M. and Stegun, I. A. (1965). *"Handbook of Mathematical Functions,"* Dover, New York.

Abrams, A. (1975). "The Influence of Fluid Viscosity, Interfacial Tension, and Flow Velocity on Residual Oil Saturation Left by Waterflood," *Soc. Petr. Eng. J.,* Vol. 15, pp. 437-447.

Barton, N. R. (1972). "A Model Study of Air Transport from Underground Openings Situated Below Groundwater Level," Proceedings, Symposium International Society for Rock Mechancs, Stuttgart, pp. T3-A1-T3-A20.

Bawden, W. F. and Roegiers, J. C. (1985). "Gas Escape from Underground Mined Storage Facilities - A Multiphase Flow Phenomenon", Proceedings, International Symposium on Fundamentals of Rock Joints, Björkliden, pp. 503-514.

Bodvarsson, G. S., Pruess, K., Stefansson, V., Björnsson, S. and Ojiambo, S. B. (1987). "East Olkaria Geothermal Field, Kenya. 1. History Match with Production and Pressure Decline Data", *J. of Geoph. Res., 92,* (B1) 521-539.

Brooks, R. H. and Corey, A. T. (1964). "Hydraulic Properties of Porous Media", Hydrol. Paper 3, Civ. Eng. Dept., Colorado State University, Fort Collins, CO., 27 pp.

Brown, S. R. (1987). "Fluid Flow Through Rock Joints: The Effect of Surface Roughness", *Journal of Geophys. Res., 92,* (B2) 1337-1347.

Brown, S. R. and Scholz, C. H. (1985). "Broad Bandwidth Study of the Topography of Natural Rock Surfaces", *Journal of Geophys. Res., 90,* 12,575-12,582.

Carslaw, H. S. and Jaeger, J. C. (1959). *"Conduction of Heat in Solids,"* Oxford University Press, Oxford, England, Second Ed.

Corey, A. T. (1954). "The Interrelation Between Gas and Oil Relative Permeabilities", *Producers Monthly,* pp. 38-41.

de Marsily, G. (1986). ''Quantitative Hydrogeology'', Academic Press, Orlando, FL.

Duff, I. S. (1977). ''MA28 - A Set of FORTRAN Subroutines for Sparse Unsymmetric Linear Equations'', AERE Harwell Report R8730.

Evans, D. D. (1983). ''Unsaturated Flow and Transport through Fractured Rock - Related to High-Level Waste Repositories'', Final Report - Phase I, Department of Hydrology and Water Resources, University of Arizona, prepared for U. S. Nuclear Regulatory Commission, Report NUREG/CR-3206.

Evans, D. D. and Huang, C. H. (1983). ''Role of Desaturation on Transport through Fractured Rock'', *in* Role of the Unsaturated Zone in Radioactive and Hazardous Waste Disposal, J. W. Mercer, P. S. C. Rao, and I. W. Marine (editors), Ann Arbor Science, pp. 165-178.

Firoozabadi, A. and Hauge, J. (1989). ''Capillary Pressure in Fractured Porous Media'', paper SPE-18747, presented at the SPE California Regional Meeting, Bakersfield, CA.

Forsythe, G. E. and Wasow, W. R. (1960). *Finite-Difference Methods for Partial Differential Equations,* John Wiley and Sons, Inc., New York, London.

Fulcher, R. A., Ertekin, T. and Stahl, C. D. (1985). ''Effect of Capillary Number and Its Constituents on Two-Phase Relative Permeability Curves'', *J. Petr. Tech., 2,* pp. 249-260.

Gale, J. E. (1987). ''Comparison of Coupled Fracture Deformation and Fluid Flow Models with Direct Measurements of Fracture Pore Structure and Stress-Flow Properties'', Proceedings, 28th U. S. Symposium on Rock Mechanics, Tucson, AZ, pp. 1213-1222.

Gentier, S. (1986). Morphologie et Comportement Hydromécanique d'une Fracture Naturelle dans un Granite Sous Contrainte Normale, Doctoral Thesis, Université d'Orléans, Orléans, France.

Gentier, S., Billaux, D. and van Vliet, L. (1989). ''Laboratory Testing of the Voids of a Fracture'', to appear in *Int. Jour. Rock Mech. and Rock. Eng.*

Gilman, J. R. and Kazemi, H. (1983). "Improvements in Simulation of Naturally Fractured Reservoirs", *Soc. Petr. Eng. J.,* pp. 695-707.

Grant, M. A. (1977). "Permeability Reduction Factors at Wairakei", paper 77-HT-52, presented at AICHE-ASME Heat Transfer Conference, Salt Lake City, Utah.

Hakami, E. (1988). "Water Flow in Single Rock Joints", Licentiate Thesis, Lulea University of Technology, Lulea, Sweden.

Heiba, A. A., Sahimi, M., Scriven, L. E. and Davis, H. T. (1982). "Percolation Theory of Two-Phase Relative Permeability", paper SPE-11015, presented at SPE 57th Annual Fall Technical Conference and Exhibition, New Orleans, LA.

Honarpour, M., Koederitz, L. and Harvey, A. H. (1986). "Relative Permeability of Petroleum Reservoirs", CRC Press, Boca Raton, FL.

Johnson, E. F., Bossler, D. P. and Narmann, V. O. (1959). "Calculation of Relative Permeability from Displacement Experiments", *Trans., AIME, 216,* 370-376.

Labastie, A., Guy, M., Delclaud, J. P. and Iffly, R. (1980). "Effect of Flow Rate and Wettability on Water-Oil Relative Permeabilities and Capillary Pressure," paper SPE-9236, presented at the 55th Annual Fall Technical Conference and Exhibition of the SPE, Dallas, TX, Sept. 1980.

Leverett, M. C. (1941). "Capillary Behavior in Porous Solids", AIME Trans., Vol. 142, p. 152.

Merrill, L. S., Jr. (1975). "Two-Phase Flow in Fractures," Ph.D. thesis, University of Denver, CO.

Montazer, P., F. Thamir and P. Harrold (1988). "Anisotropic Relative Permeability in a Plane Fracture", paper presented at International Conference on Fluid Flow in Fractured Rocks, Atlanta, GA.

Narasimhan, T. N. and Witherspoon, P. A. (1976). "An Integrated Finite Difference Method for Analyzing Fluid Flow in Porous Media", *Water Resources Research,* Vol. 12, No. 1, pp. 57-64.

Osoba, J. S., Richardson, J. G., Kerner, J. K., Hafford, J. A. and Blair, P. M. (1951). "Laboratory Measurements of Relative Permeability", *Pet. Trans., AIME*, 47-55.

Peaceman, D. W. (1977). "Fundamentals of Numerical Reservoir Simulation", Elsevier, Amsterdam.

Pruess, K. (1983). "Development of the General Purpose Simulator MULKOM", Annual Report 1982, Earth Sciences Division, Lawrence Berkeley Laboratory Report LBL-15500.

Pruess, K. (1988). "SHAFT, MULKOM, TOUGH: A Set of Numerical Simulators for Multiphase Fluid and Heat Flow", *Geotermia, Rev. Mex. Geoenergia, 4,* (1) 185-202 (also: Lawrence Berkeley Laboratory Report LBL-24430).

Pruess, K. (1989). "Modeling Studies of Multiphase Fluid and Heat Flow Processes in Nuclear Waste Isolation", *in* W. Lutze and R. C. Ewing (eds.), Scientific Basis for Nuclear Waste Management XII, Materials Research Society Symposium Proceedings, Vol. 127, pp. 793-803, Pittsburgh, PA.

Pruess, K., Bodvarsson, G. S. and Stefansson, V. (1983). "Analysis of Production Data from the Krafla Geothermal Field, Iceland", paper presented at Ninth Workshop on Geothermal Reservoir Engineering, Stanford University, Stanford, CA.

Pruess, K., Bodvarsson, G. S., Stefansson, V. and Eliasson, E. T. (1984). "The Krafla Geothermal Field, Iceland, 4. History Match and Prediction of Individual Well Performance", *Water Resources Research, 20,* (11) 1561-1584.

Pruess, K., Wang, J. S. Y. and Tsang, Y. W. (1988). On Thermohydrological Conditions near High-Level Nuclear Wastes Emplaced in Partially Saturated Fractured Tuff. Part 2. Effective Continuum Approximation, Lawrence Berkeley Laboratory Report LBL-24564, January. (To appear in *Water Resources Research.)*

Pyrak-Nolte, L. J., Cook, N. G. W. and Nolte, D. D. (1988). "Fluid Percolation Through Single Fractures", Geophys. Res. Lett., Vol. 15, No. 11, pp. 1247-1250.

Pyrak-Nolte, L. J., Myer, L. A., Cook, N. G. W., and Witherspoon, P. A. (1987). "Hydraulic and Mechanical Properties of Natural Fractures in Low Permeability Rock", paper presented at Sixth International Congress on Rock Mechanics, Montreal, Canada, August.

Rasmussen, T. C. (1987). "Computer Simulation Model of Steady Fluid Flow and Solute Transport through Three-Dimensional Networks of Variably Saturated, Discrete Fractures", *in* D. D. Evans and T. J. Nicholson (eds.), Flow and Transport through Unsaturated Fractured Rock, Geophysical Monograph 42, American Geophysical Union, pp. 107-114.

Rasmussen, T. C., C. H. Huang and D. D. Evans (1985). "Numerical Experiments on Artificially-Generated, Three-Dimensational Fracture Networks: An Examination of Scale and Aggregation Effects", *in* International Association of Hydrogeologists (ed.), Memoirs, Vol. XVII, pp. 676-682.

Romm, E. S. (1966). "Fluid Flow in Fractured Rocks," Moscow (translated by W. R. Blake, Bartlesville, OK, 1972).

Scheidegger, A. E. (1974). "The Physics of Flow Through Porous Media" University of Toronto Press, Toronto and Buffalo, 3rd Edition.

Tsang, Y. W. and Hale, F. V. (1988). "A Study of the Application of Mercury Porosimetry Method to a Single Fracture," paper presented at the International Conference on Fluid Flow in Fractured Rocks, Atlanta, GA, May 1988.

Tsang, Y. W. and Tsang, C. F. (1987). "Channel Model of Flow through Fractured Media", *Water Resources Res., 23,* (3) 467-479, March.

Verma, A. K. (1986). Effects of Phase Transformation on Steam-Water Relative Permeabilities, Doctoral Dissertation, University of California, Berkeley, CA, March (also: Lawrence Berkeley Laboratory Report LBL-20594).

Wang, J. S. Y., Narasimhan, T. N. and Scholz, C. H. (1988). "Aperture Correlation of a Fractal Fracture", *Journal Geophys. Res., 93,* (B3) 2216-2224.

Weber, K. J. and Bakker, M. (1981). "Fracture and Vuggy Porosity", paper SPE 10332, presented at the 56th Annual Fall Technical Conference and Exhibition of the SPE, San Antonio, TX.

Williams, S. A. and El-Kadi, A. I. (1986). COVAR - A Computer Program for Generating Two-Dimensional Fields of Autocorrelated Parameters by Matrix Decomposition, Report, International Groundwater Modeling Center, Holcomb Research Institute, Butler University, Indianapolis, Indiana.

Yanosik, J. L., and McCracken, T. A. (1979). "A Nine-Point, Finite Difference Reservoir Simulator for Realistic Prediction of Adverse Mobility Ratio Displacements", *Soc. Pet. Eng. J.*, 253-262.

APPENDIX

Capillary pressure versus saturation relationship for a lognormal aperture distribution

Given an aperture distribution for a rough-walled fracture, and assuming that regardless of the spatial arrangement of the apertures, they are filled by the wetting phase in ascending order up to a cutoff aperture b_c, we may write the saturation of the wetting phase $S_w(b_c)$ as

$$S_w(b_c) = \frac{\int_0^{b_c} bn(b)db}{\int_0^{\infty} bn(b)db} \tag{A1}$$

For a lognormal distribution

$$n(b)db = \tilde{n}(u)du = \frac{1}{\sqrt{2\pi\sigma^2}} \exp -\frac{(u-u_o)^2}{2\sigma^2} du \tag{A2}$$

where $\tilde{n}(u)$ is the normal distribution, and

$$\begin{aligned} u &= \log b \\ u_o &= \log b_o \end{aligned} \tag{A3}$$

Expressed in terms of u, Eq. (A1) becomes

$$S_w(b_c) = \frac{\int_{-\infty}^{\log b_c} e^{u\ln 10} \tilde{n}(u)du}{\int_{-\infty}^{\infty} e^{u\ln 10} \tilde{n}(u)du} \tag{A4}$$

Integrating (A4) yields:

$$S_w(b_c) = \frac{1}{2} \mathrm{erfc} \left[\frac{v - \log b_c}{\sqrt{2\sigma^2}} \right] \tag{A5}$$

Where $v = \sigma^2 \ln 10 + \log b_o$, and $\mathrm{erfc}(x) = 1 - \mathrm{erf}(x)$ is the complementary error function (Carslaw and Jaeger, 1959; Abramowitz and Stegun, 1965).

	Case 1	Case 2
mean aperture (μm)	81.8	81.8
standard deviation	0.43	0.43
x-spatial correlation	0.20	0.60
y-spatial correlation	0.20	0.20

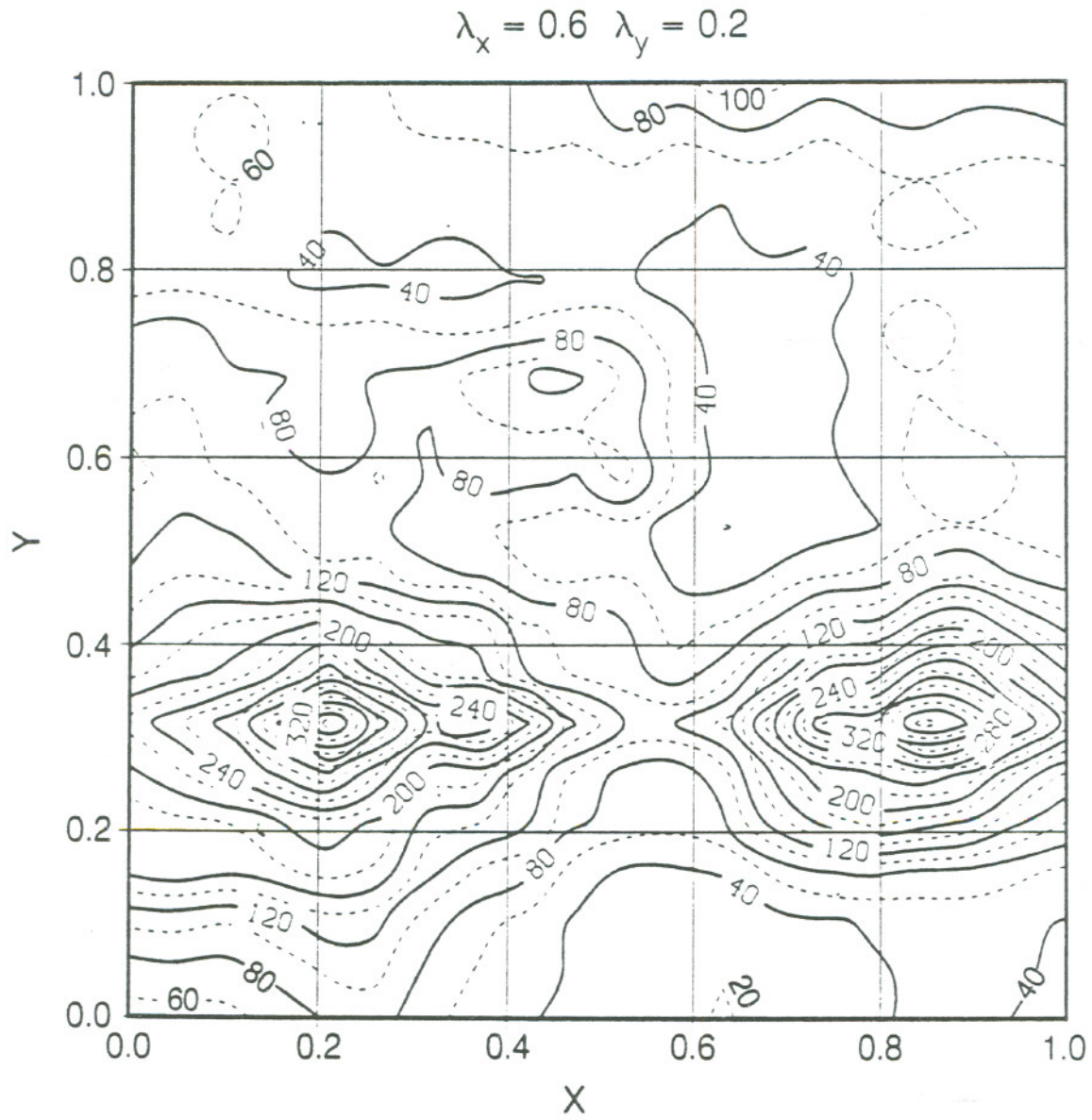Table 1.   Parameters for lognormal aperture distributions
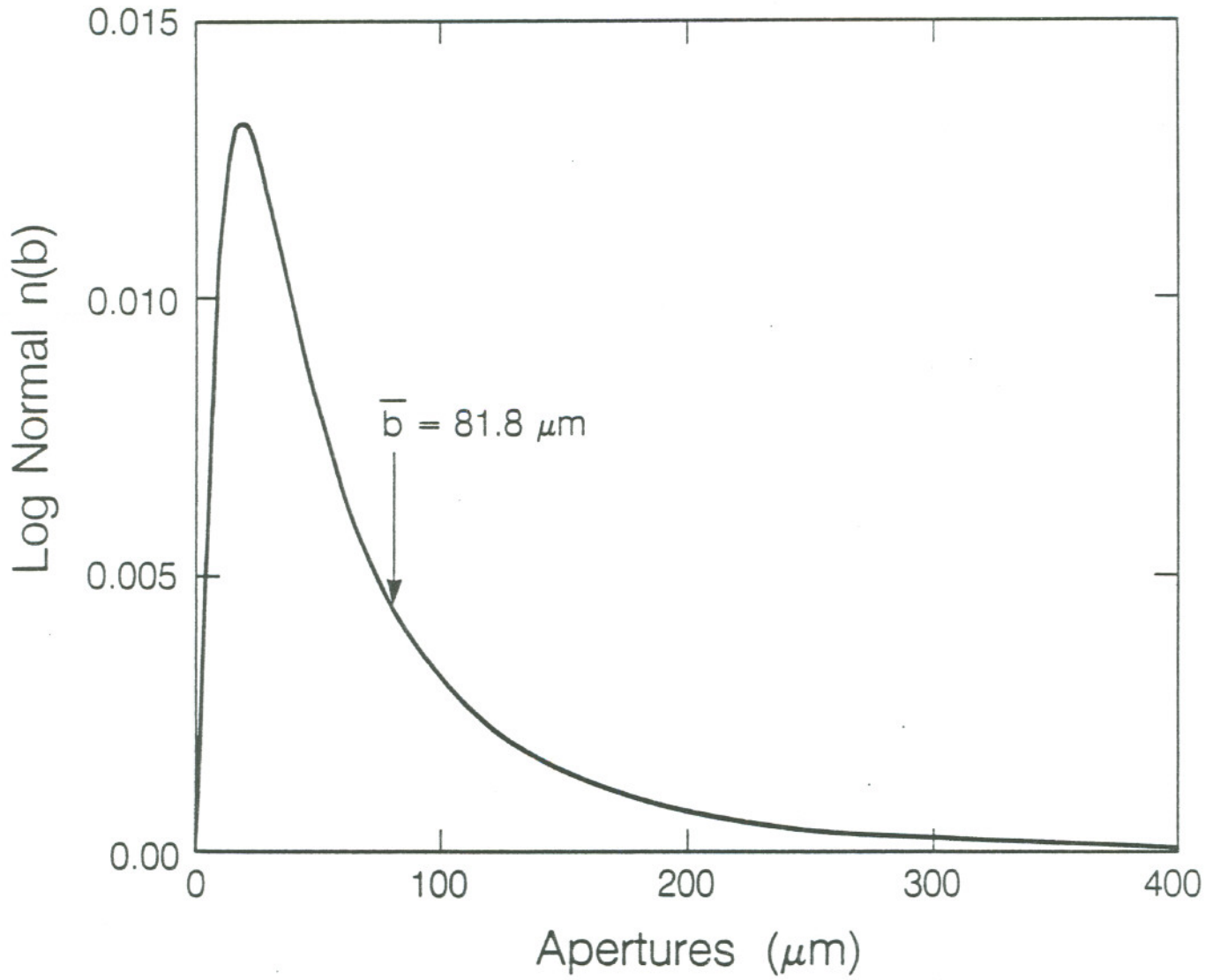
Figure 1.   Lognormal aperture distribution with a mean aperture of 81.8 μm and a standard deviation of 0.43.
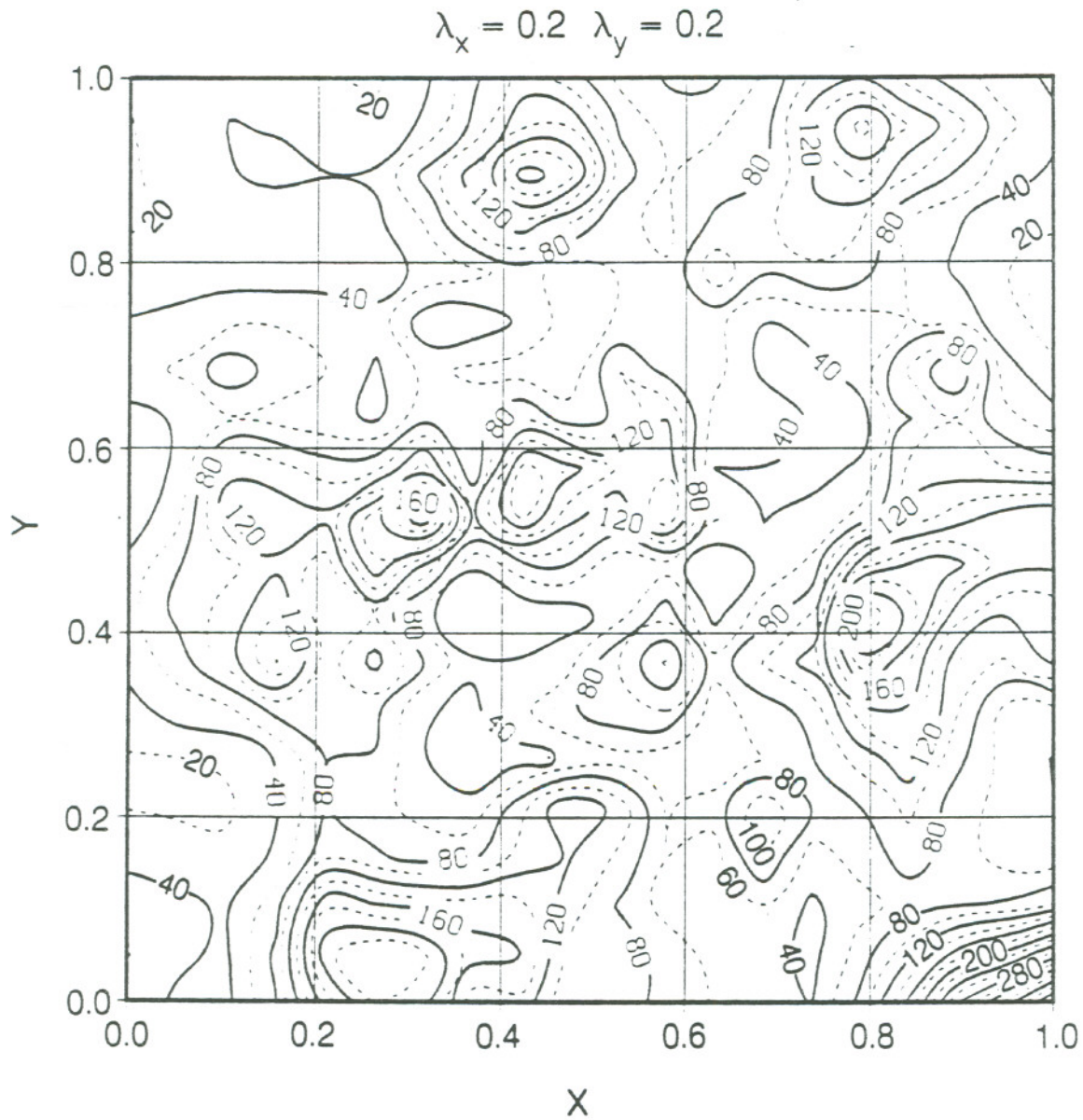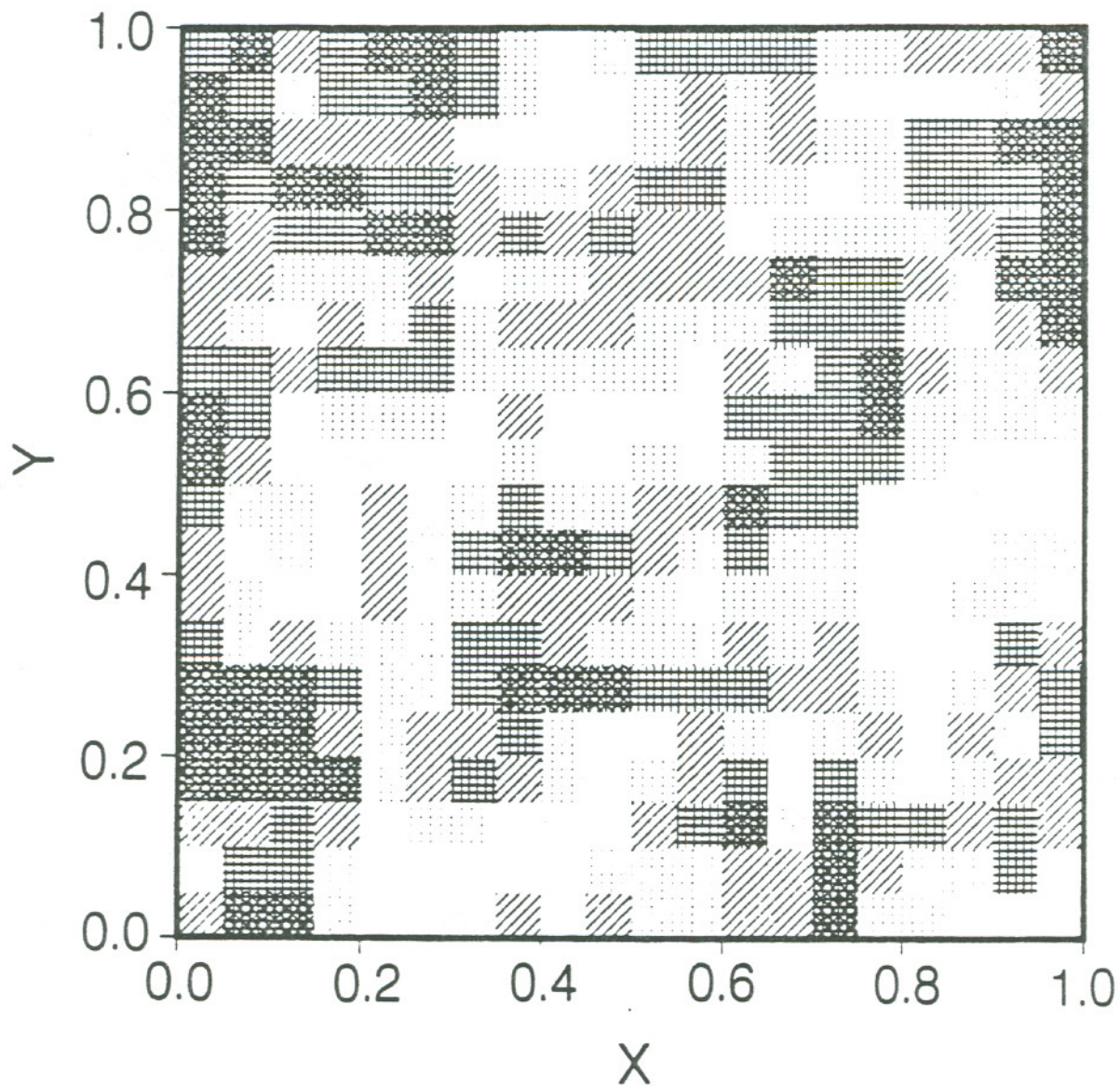
XBL 891-7444

Figure 2.   Contour diagram of a lognormal aperture distribution in a fracture plane with isotropic spatial correlation (Case 1, Table 1; units on contour lines are μm).

$$\lambda_x = 0.6 \quad \lambda_y = 0.2$$

XBL 891-7412

Figure 3.   Contour diagram of a lognormal aperture distribution with anisotropic spatial correlation (Case 2, Table 1; units on contour lines are μm).

$$\lambda_x = 0.2 \quad \lambda_y = 0.2$$

XBL 891-7414

Figure 4. A 20 x 20 discretized version of the fracture apertures shown in Figure 2. The magnitudes of the apertures are indicated by shading, with lighter shading corresponding to larger aperture.

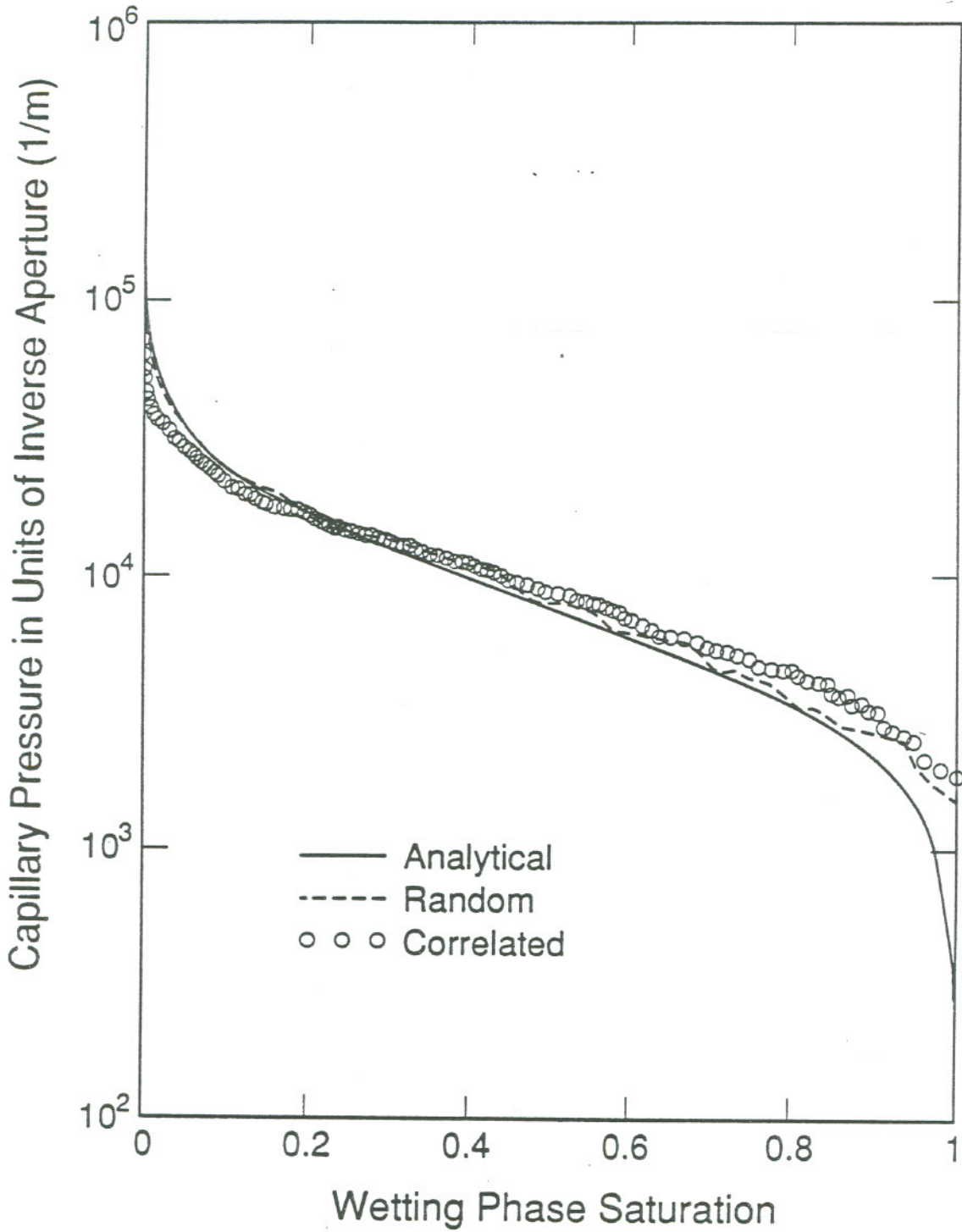$$\lambda_x = 0.6 \quad \lambda_y = 0.2$$
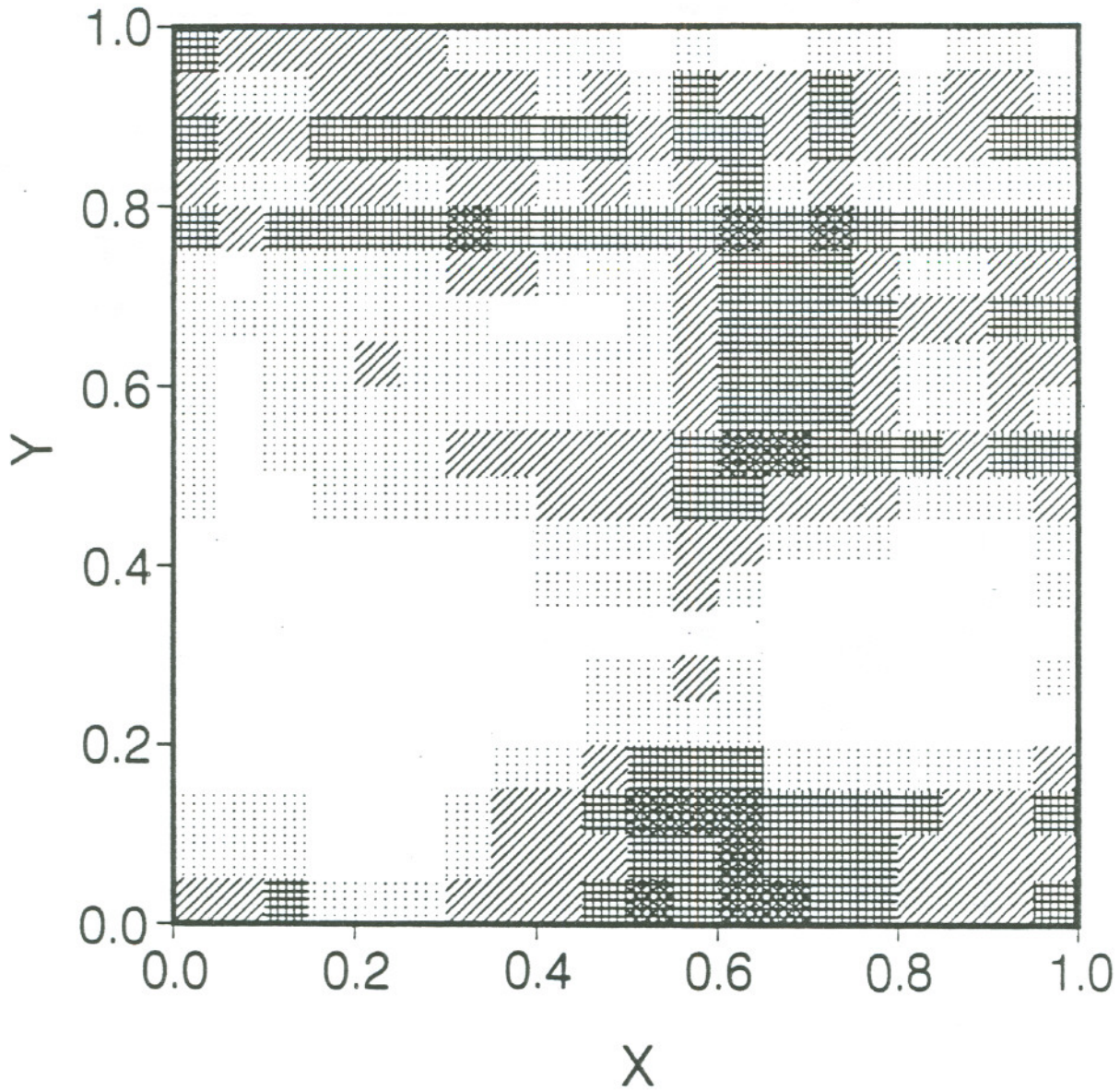
XBL 891-7415

Figure 5. A 20 x 20 discretized version of the fracture apertures shown in Figure 3.
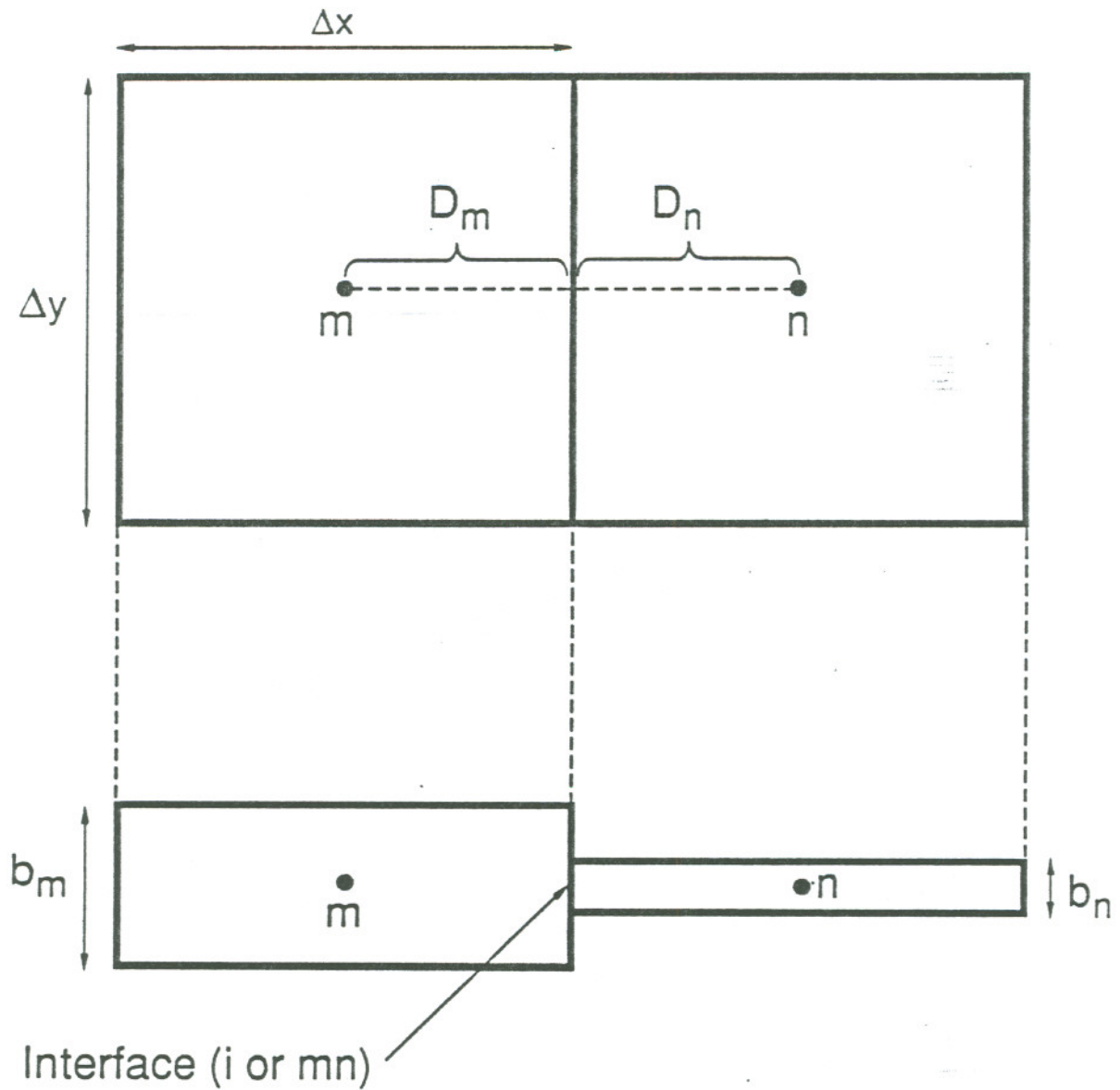
Figure 6. Schematic of a connection between two fracture elements, looking down onto the fracture plane (top), and giving an elevation view (bottom).
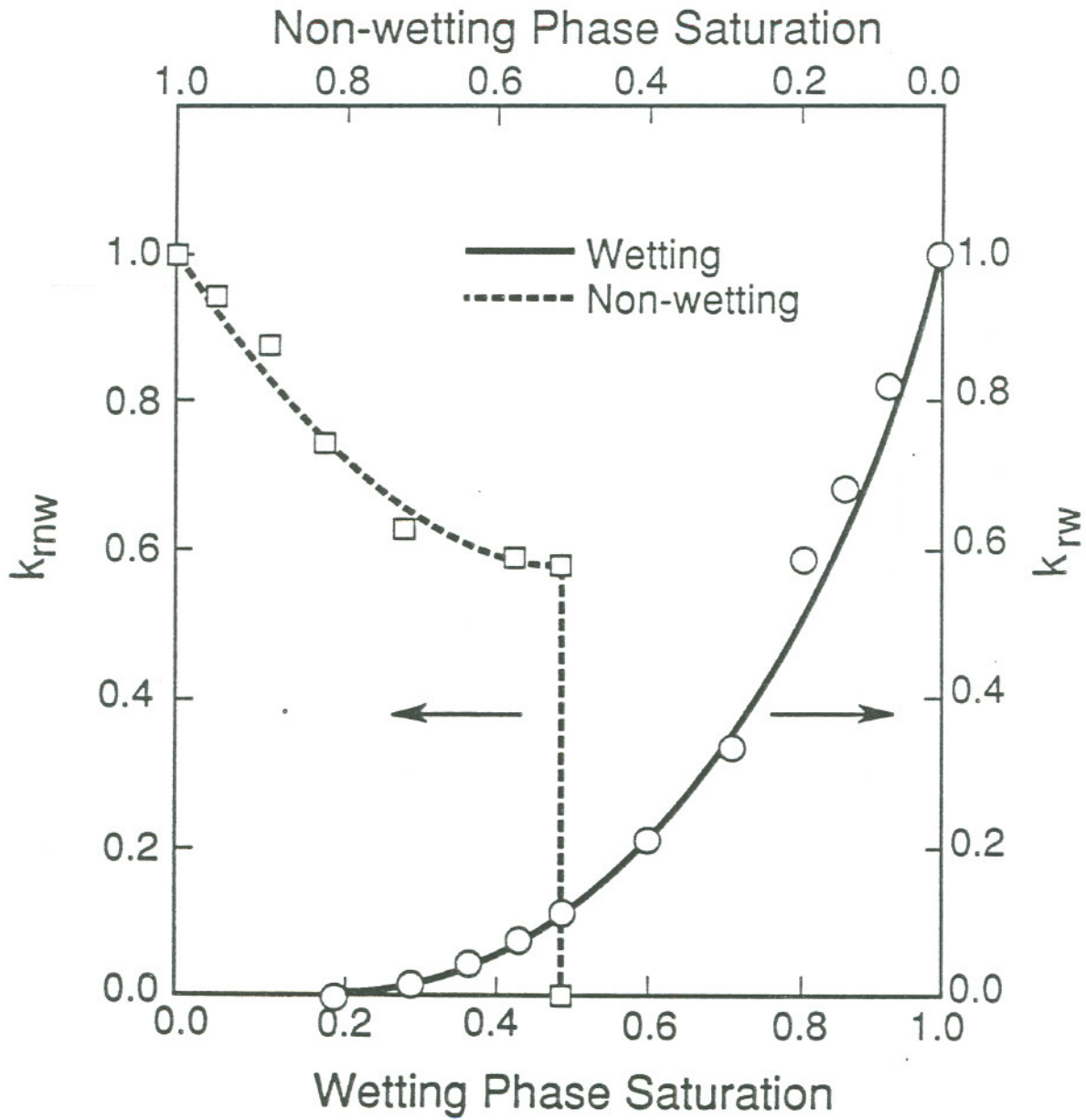
XBL 896-7637

Figure 7.   Capillary pressure (in units of inverse aperture) versus saturation relation-
ship for fracture with lognormal aperture distribution. The different curves
are explained in the text.
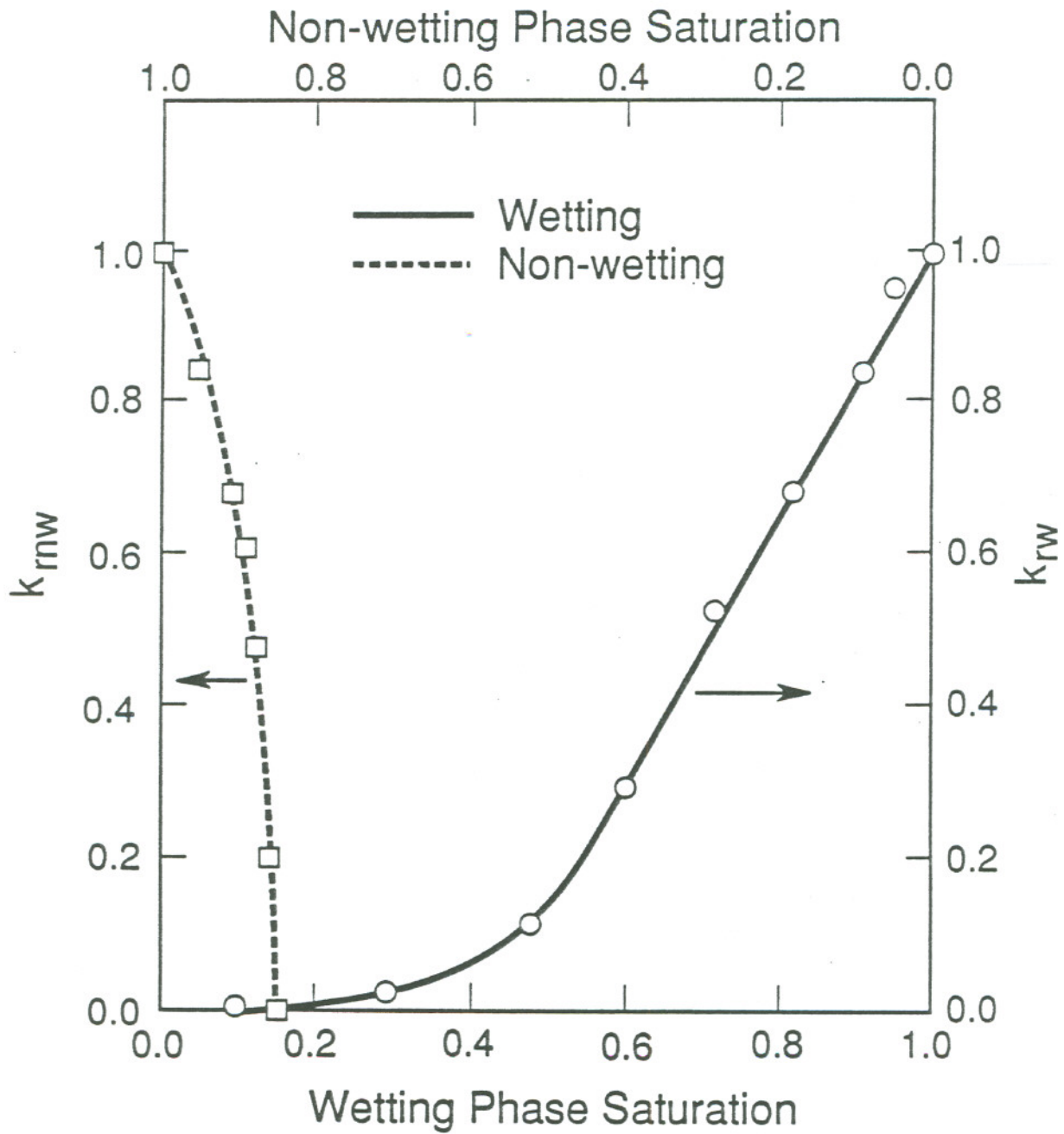
XBL 891-7043

Figure 8. Simulated wetting and nonwetting phase relative permeabilities for the log-
normal aperture distribution of Figures 1 and 3.

Figure 9.   Simulated wetting and nonwetting phase relative permeabilities for the log-normal aperture distribution of Figures 2 and 4 with long-range anisotropic spatial correlation.